horticulturae

MDPI

Article

Genome-Wide Characterization of Class III Peroxidases and Their Expression Profile During Mycorrhizal Symbiosis and Phosphorus Deprivation in Lettuce (*Lactuca sativa* L.)

Samuel Simoni †, Marco Castellacci †, Gabriele Usai, Ugo Rogo, Flavia Mascagni, Tommaso Giordani, Lucia Natali, Andrea Cavallini and Alberto Vangelisti *

Department of Agriculture, Food and Environment (DAFE), University of Pisa, Via del Borghetto 80, 56124 Pisa, Italy

* Correspondence: alberto.vangelisti@unipi.it

† These authors contributed equally to this work.

Abstract: Lettuce cultivation requires high fertilizer inputs, which impact the environment and costs. Arbuscular mycorrhizal symbiosis (AMS) can reduce fertilizer use, enhance plant nutrition (especially phosphorus), and promote healthier plants. Class III peroxidases (PRXs) play crucial roles in various physiological processes and stress responses. However, their role in AMS and phosphorous (P) deficiency is still unclear. Our study identified 91 *PRX* genes in the lettuce genome (*LsPRXs*) and clustered them into eight subfamilies based on phylogenetic relationships. Evolutionary analysis indicated that tandem duplication was the main driver for *LsPRX* gene family expansion. Synteny analysis showed orthologous relationships of the *PRX* gene family between lettuce and potato, Arabidopsis, and maize, identifying 39, 28, and 3 shared PRXs, respectively. Transcriptomic data revealed that most *LsPRX* genes were more expressed in roots than in leaves and differentially expressed *LsPRXs* were found in response to AMS and P supply. Notably, 15% of *LsPRX* genes were differentially expressed in roots during mycorrhization. Gene expression network analysis highly correlated five *LsPRXs* (*LsPRX17*, *LsPRX23*, *LsPRX24*, *LsPRX64*, and *LsPRX79*) with genes involved in cell wall remodeling and reorganization during mycorrhization. Our results provide insights into the evolutionary history and functional roles of *PRX* genes in lettuce and identify candidate gene targets that may enhance the bio-stimulant effects of AMS and help to cope with P deficiency.

Keywords: peroxidases; lettuce; arbuscular symbiosis; phosphate deficiency; transcriptomics; gene family

check for updates

Citation: Simoni, S.; Castellacci, M.; Usai, G.; Rogo, U.; Mascagni, F.; Giordani, T.; Natali, L.; Cavallini, A.; Vangelisti, A. Genome-Wide Characterization of Class III Peroxidases and Their Expression Profile During Mycorrhizal Symbiosis and Phosphorus Deprivation in Lettuce (*Lactuca sativa* L.). *Horticulturae* **2024**, *10*, 1170. https://doi.org/10.3390/horticulturae10111170

Academic Editor: Xiaowu Wang

Received: 23 September 2024
Revised: 18 October 2024
Accepted: 2 November 2024
Published: 5 November 2024

Copyright: © 2024 by the authors. Licensee MDPI, Basel, Switzerland. This article is an open access article distributed under the terms and conditions of the Creative Commons Attribution (CC BY) license (https://creativecommons.org/licenses/by/4.0/).

1. Introduction

Peroxidases (PRXs) represent a broad and diverse family of enzymes that facilitate the oxidation of a wide range of electron donor substrates. These enzymes are ubiquitously distributed in nature and are involved in numerous aspects of plant growth and physiology [1,2]. Due to their critical biological functions, PRXs have been extensively studied, with numerous research efforts aiming to characterize this enzyme family for various applications, including their use as biological markers and in diagnostic assays [3]. PRXs are classified into three main groups based on their sequences and catalytic activities. Class I peroxidases, which are present in most living organisms except animals, play a crucial role in detoxifying excess hydrogen peroxide (H_2O_2). This class includes catalases, ascorbate–peroxidases, and cytochrome *c*-peroxidases [4]. The class II peroxidases are primarily produced by fungi and are predominantly involved in the degradation of soil debris [5]. Class III peroxidases, the largest group, consist of a multigenic family mostly found in the plant kingdom. These enzymes are associated with a multitude of physiological processes [6] and stages of the plant life cycle [7]. For instance, class III peroxidases are key players in cell wall biosynthesis [1], lignification [8], regulation of the auxin pathway [9], reactive oxygen species (ROS) detoxification [10], and defense against pathogens [11].

These enzymes are encoded by a large multigenic family, with substantial numbers of gene members identified in various plant species, such as Arabidopsis, maize, and potato, with 73, 119, and 102 *PRXs* class III genes, respectively [12–14]. Despite the well-documented association of class III PRXs with several plant biological processes, many roles of this multigenic family, such as in arbuscular mycorrhizal symbiosis (AMS) and phosphorus (P) deprivation, remain to be elucidated [15].

Phosphorus is an indispensable but environmentally limiting macronutrient central to energy transfer and metabolic regulation. It is a key structural constituent of essential biomolecules such as phospholipids, nucleic acids, sugar phosphates, and adenylates and plays a crucial role in protein synthesis [16–18]. Although P is vital for plant growth and productivity, its availability is often insufficient for optimal plant development due to soil fixation [19]. A common strategy to address crop phosphorus deficiency is to apply large quantities of phosphorus fertilizers. However, accessible global reserves of P are projected to be largely depleted by the end of this century [18].

AMS is an area of emerging interest and represents a mutualistic association at the root level between plants and mycorrhizal fungi (AMF) of the subphylum Glomeromycotina [20]. The AMS facilitates a beneficial exchange of nutrients, wherein fungi enhance nitrogen and P uptake from the soil through an extensive network of extraradical hyphae in exchange for fatty acids and sugars from the plant [21]. This interaction optimizes nutrient exchange but also promotes plant growth, enhances adaptation to various biotic and abiotic stresses, strengthens plant defense mechanisms, and boosts the production of primary and secondary metabolites [22,23]. From an agronomic perspective, AMS has been shown to reduce the requirement for P fertilization without compromising crop yield [24]. This aspect represents a significant advantage, as it mitigates the environmental impact of P exploitation, a resource that is both costly and non-renewable [25]. Over the past decade, molecular studies on AMS have revealed extensive transcriptome remodeling, particularly involving genes associated with transcription factors, hormonal regulation, primary and secondary metabolism, transporters, and ROS scavenging mechanisms [26,27]. These changes occur not only at the root level but also in leaves and fruits [28,29]. Recent investigations into the effects of AMS under P deprivation in lettuce have demonstrated notable improvements in growth, photosynthesis, and the production of primary and secondary metabolites [30]. These results are accompanied by a comprehensive rearrangement of gene expression profiles in both roots and leaves [31,32].

Lettuce (*Lactuca sativa* L.), an autogamous plant belonging to the Asteraceae family, is extensively cultivated, with over one million hectares yielding 27 million tons globally in 2022 (FAOSTAT data https://www.fao.org/faostat/en/#data/QCL; accessed on 15 January 2024). Lettuce holds significant economic value and includes seven primary cultivar groups renowned for their high concentrations of vitamins and secondary metabolites [33]. From a genomic point of view, lettuce is well characterized, with a fully sequenced genome of 2.6 Gb across nine chromosomes (2n = 2x = 18), encompassing approximately 50,000 genes [34], making it an ideal candidate for gene family characterization.

Although class III PRXs have been characterized in several crop species and linked to various biological processes, their roles in the bio-stimulating effects of AMS and P deprivation of economically valuable crops such as lettuce remain largely unexplored. Therefore, our study aims to characterize at a genome-wide scale the class III *PRX* multigenic family in *L. sativa* for the first time, elucidating their expression patterns and functional roles by comparing lettuce plants (cv. Salinas) grown hydroponically at suboptimal P concentration (0.5 mM) and inoculated with the AM fungus *Funneliformis mosseae* (LoP/+AM) with non-inoculated plants grown at optimal (1.0 mM; HiP/−AM) P concentration. Our analysis has uncovered the number and evolution of the PRX family in lettuce and has highlighted their role in plant–fungus bio-stimulation, suggesting that *PRXs* could also be key target genes for crop genetic improvement.

2. Materials and Methods

2.1. Identification of PRX Genes

The protein sequences of the Arabidopsis (*A. thaliana*) class III PRX (AtPRX) genes [12] were downloaded from the Arabidopsis database [35] (https://www.arabidopsis.org; accessed on 22 January 2024). The AtPRX proteins were used as query by a blastp search using BLAST tool v2.6.0+ [36] to identify the PRX orthologs in lettuce proteome (*L. sativa* cv. Salinas [34]; BioProject PRJNA173551), downloaded from the National Center for Biotechnology Information (NCBI, https://www.ncbi.nlm.nih.gov/datasets/genome; accessed on 22 January 2024). The resulting proteins, with more than 40% similarity and an e-value < 1×10^{-10}, were considered putative LsPRXs. The occurrence of the PRX protein domain PF00141 was confirmed by InterProScan [37] using the Pfam v23.0 database and successively confirmed using the Conserved Domain Database of NCBI (https://www.ncbi.nlm.nih.gov/cdd; accessed on 22 January 2024).

2.2. Structural and Genomic Characterization of LsPRX Sequences

The LsPRXs phylogenetic tree was constructed by MEGA X v10.1.8 [38] using the maximum likelihood parameter with a total of 1000 bootstrap replications on the Jones, Taylor, and Thornton (JTT) amino acid substitution model. The *LsPRX* exon–intron gene structures were identified using the Gene Structure Display Server (GSDS v2.0; http://gsds.gao-lab.org; accessed on 25 January 2024). The LsPRX conserved motifs were investigated using MEME v5.5.5 [39] with default parameters, except for the "number of motifs," set to 20. The putative promoter regions at 1000 bp upstream of each *LsPRX* gene were investigated using the PlantCARE database [40]. The P1BS cis-element, not detected by PlantCARE, was identified by aligning the *LsPRX* promoter regions with the motif (GNATATNC) using Clustal Omega (https://www.ebi.ac.uk/jdispatcher/msa/clustalo; accessed on 25 January 2024).

2.3. LsPRX Chromosomal Distribution and Gene Duplication Events

The duplication events that occurred in the *LsPRX* gene family were analyzed using MCScanX v1.0 [41] using the parameters e-value < 1×10^{-10} and -max_target_seqs 5. Events involving duplicated *LsPRX* genes were identified from the collinearity file using the Perl script "detect_collinearity_within_gene_families" provided by MCScanX. The "RIdeogram" R package was used to display the *LsPRX* distribution in lettuce chromosomes with the parameter "window = 1,000,000" [42].

2.4. Phylogenetic and Collinearity Analysis of PRX Proteins Among Species

LsPRX protein sequences were aligned with other known PRX proteins of Arabidopsis, maize (*Z. mays*), and potato (*S. tuberosum*) reported in previous studies [12,14,43]. The alignment was performed using Muscle within MEGA X, with default parameters. The phylogenetic tree of PRX belonging to all species was constructed on MEGA X using the maximum likelihood parameter with a total of 1000 bootstrap replications based on the JTT amino acid substitution model. All protein sequences and gff3 files of Arabidopsis (BioProject PRJNA10719), maize (BioProject PRJNA655717), and potato (BioProject PRJNA225997) were downloaded from the NCBI (https://www.ncbi.nlm.nih.gov/datasets/genome; accessed on 22 January 2024) to conduct the syntenic analysis. The syntenic maps were constructed using One Step MCScanX in TBtools v2.057 with default parameters [44]. Amazing Super Circos in TBtools was used to display the gene localization and the syntenic blocks between the chromosomes with default parameters.

2.5. LsPRX Expression and Gene Network Analysis

The lettuces used in the experiment were the same as those used in two previous works [30,32]. Briefly, the expression of *PRX* genes in relation to AMS was studied in a completely randomized experiment as follows: (1) lettuces inoculated with *F. mosseae* and grown in sub-optimal phosphate concentration (0.5 mM) nutrient solution (LoP/+AM), (2) lettuces grown in sub-optimal P concentration (0.5 mM) without mycorrhizal inter-

action (LoP/−AM), and (3) and lettuces grown in optimal (1 mM) P concentration in the nutritive solution (HiP/−AM) [32]. Three biological replicates of Illumina RNA-seq libraries from leaf and root samples of *L. sativa*, harvested from LoP/−AM, LoP/+AM, and HiP/−AM plants, were downloaded from the Sequence Read Archives (SRA) (Bioproject PRJNA1043852).

Global read quality was assessed using FastQC v0.11.9 (https://www.bioinformatics.babraham.ac.uk/projects/fastqc/; accessed on 22 January 2024) and subsequently improved with Trimmomatic v0.39 [45] using the following parameters: SLIDINGWINDOW: 4:24, CROP: 120, HEADCROP: 20, MINLEN: 120. Ribosomal sequences were removed from high-quality cDNA libraries by aligning reads to lettuce rRNA downloaded from the SILVA database [46]. Sequence alignment was performed using CLC Genomic Workbench v9.5.3 (CLC-BIO, Aarhus, Denmark) with the following parameters: mismatch cost = 2, insertion/deletion cost = 3, length fraction = 0.5, and similarity fraction = 0.8. The resulting high-quality reads were mapped to the lettuce transcriptome using CLC Genomic Workbench with the following parameters: mismatch penalties = 2, gap open penalties = 3, length fraction = 0.9, and similarity fraction = 0.9. Gene-specific reads were normalized using reads per kilobase of transcript per million reads mapped (RPKM) [47]. Differentially expressed genes (DEGs) were identified with a likelihood ratio test using EdgeR v3.28.1 [48]. Two pairwise comparisons were performed using libraries from lettuces grown in reduced P concentration (LoP/−AM) as the control: (1) LoP/−AM vs. HiP/−AM to investigate the effect of P nutrition, and (2) LoP/−AM vs. LoP/+AM to detect the effect of AM symbiosis under P deficiency [32]. Genes with an absolute fold change greater than 2 and a false discovery rate (FDR)-corrected p-value < 0.05 [49] were considered differentially expressed. The differential expression analysis excluded transcripts with an RPKM value < 1 in each library.

Expression values (RPKM) of DEGs in roots during mycorrhization were used to build the co-expression network using the R package "WGCNA" v1.68 [50]. A soft threshold power of 42 was selected as the optimal value to calculate the adjacency matrix, based on the criterion of achieving a scale-free topology. The eigengene dendrogram for module detection was constructed using the dynamic tree cut method (MEDissThres = 0.09, minModuleSize = 50). The co-expression network of genes, with a cut-off of 0.75, was visualized using VisANT v5.53 [51].

3. Results

3.1. Genome-Wide Identification of PRX Genes in Lettuce

A total of 97 PRX proteins were identified in the lettuce (*L. sativa* cv. Salinas) proteome (LsPRX proteins). The PF00141 PRX protein domain, regrouping the PRX multigene family [52], was confirmed using InterProScan with the Pfam v23.0 database, and subsequently, the putative LsPRX proteins were validated using the Conserved Domain Database (CDD) from NCBI. After filtering, 91 LsPRXs proteins were retained and renamed LsPRX1 to LsPRX91 based on their chromosomal locations (Supplementary Table S1). However, the location of LsPRX91 on the chromosome could not be determined, as it was found on an unplaced scaffold. The protein lengths of the 91 *LsPRX* genes ranged from 276 (LsPRX4) to 571 amino acids (LsPRX19), with an average length of 330.6 amino acids (Supplementary Table S1). The complete amino acid and CDS sequences of LsPRXs are available in Supplementary Data S1 and S2, respectively.

3.2. Phylogenetic, Gene Structure, Conserved Motif, and Promoter Analyses of LsPRX Gene Family

To unveil the evolutionary relationship of the *LsPRX* gene family, an unrooted phylogenetic tree (Figure 1) was constructed. The 91 *LsPRX* genes were categorized into eight groups (I-VII) based on bootstrap values (>60%) observed on the phylogenetic tree. However, 2 *LsPRX* genes (*LsPRX82* and *LsPRX41*) could not be confidently assigned to any of the eight groups due to low bootstrap values (<60%). Group I contained the largest clade, comprising 34 *LsPRX* genes, followed by group II, with 18 *LsPRX* members, and group IV,

with 15 *LsPRX* genes. These three groups collectively represented 73.6% of the total *LsPRXs*. In contrast, groups III and V each contained only two *LsPRX* genes. Structural analysis of *LsPRX* genes revealed variability in the number of exons, ranging from 1 to 4 (Figure 1a; Supplementary Figure S1a), with nine genes lacking introns (*LsPRX31*, *LsPRX32*, *LsPRX30*, *LsPRX33*, *LsPRX29*, *LsPRX28*, *LsPRX12*, *LsPRX20*, and *LsPRX39*) (Figure 1a). Although structural variation was found among *LsPRXs*, genes with similar exon/intron structures were grouped, providing further evidence of their phylogenetic relationships (Figure 1).

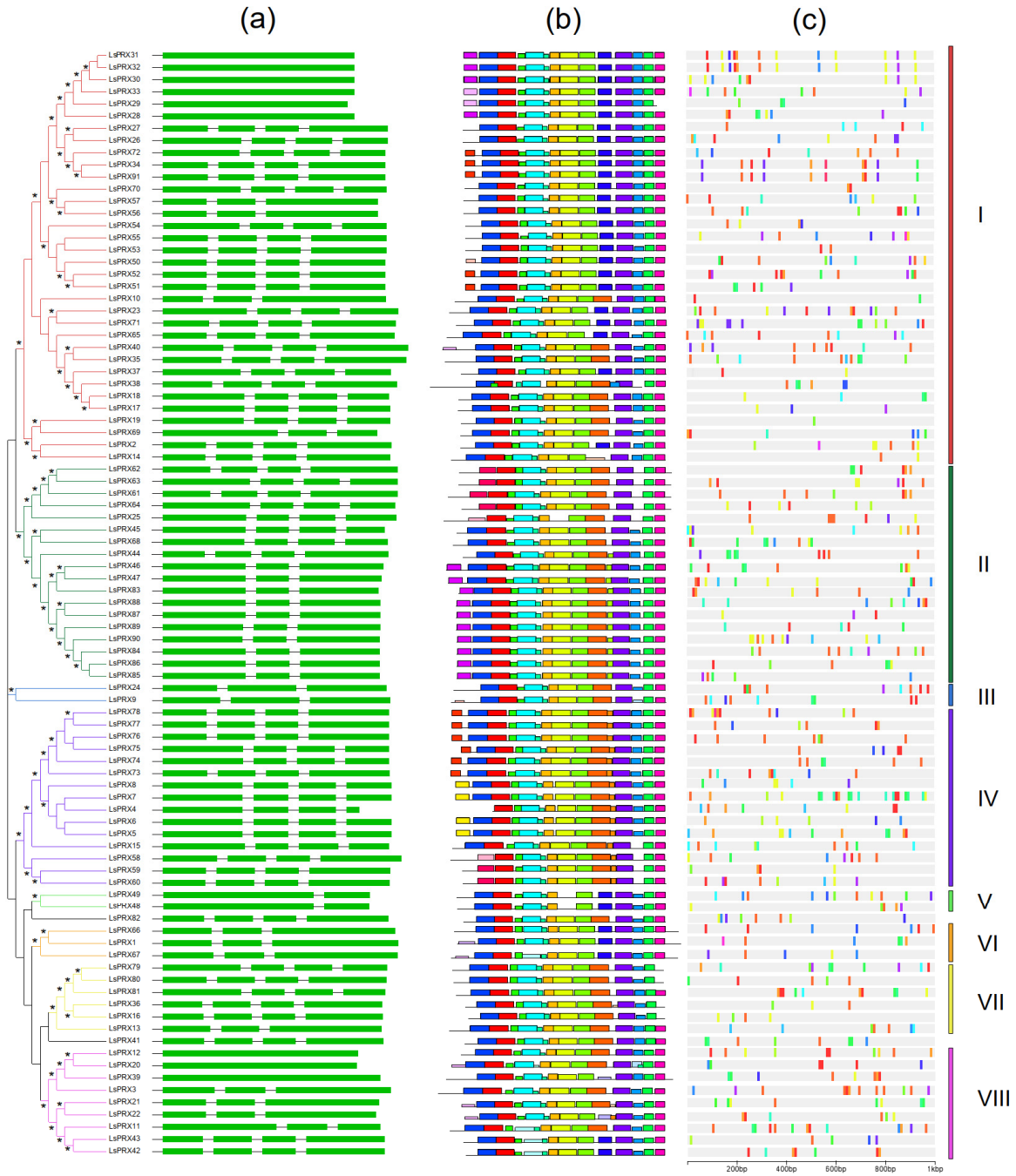

Figure 1. Phylogenetic tree, gene structure, motif distribution, and cis-elements of *LsPRX* genes. Asterisk (*) indicates bootstrap values above 60% in the phylogenetic tree of LsPRXs proteins. The roman numbers indicate PRX groups. (**a**) Exon (green) and intron (black dash) structure; (**b**) structural motifs identified on protein sequences; (**c**) loci position of predicted cis-acting elements in the 1000 bp upstream region of *LsPRX* genes. The legends for colors in (**a**–**c**) are specified in Supplementary Figure S1.

The motif distribution of the 91 LsPRX proteins was analyzed to explore the diversity of motif components. A total of 20 conserved motifs were identified (Figure 1b; Supplementary Figure S1b) [53]. In particular, motifs 1, 4, 5, 6, 9, 11, and 12 were shared among all 91 LsPRXs (Figure 1b; Supplementary Figure S1b). Furthermore, LsPRX proteins belonging to the same group exhibited similar conserved motif composition and order, suggesting that these proteins may share similar functions. However, slight variations in a few motifs characterize subgroups within some groups, such as I, II, and IV. For instance, in group II, only 10 LsPRXs (LsPRX46, LsPRX47, LsPRX83, LsPRX88, LsPRX87, LsPRX89, LsPRX90, LsPRX84, LsPRX86, and LsPRX85) contain motif 15 (QYGFYNGKCRSSDVEDIVRRTVYSKY) (Supplementary Figure S1b). A complete list of consensus motif sequences is available in Supplementary Figure S1b.

Cis-elements in *PRX* promoter regions were analyzed to investigate whether the structure is also duplicated at the level of the non-coding sequence (Figure 1c; Supplementary Figure S1c). Overall, the results identified two classes of cis-elements distributed among the *LsPRX* groups: abiotic stress response elements (light, anaerobic induction, wound, defense and stress, low temperature, drought inducibility, and anoxic specific inducibility), making up 55.5%, and hormone response elements (ABA, MeJA, GA, SA, and IAA), constituting 45.5% of the total (Supplementary Table S2). The most abundant cis-elements shared among all *LsPRXs* were related to light responsiveness (G-Box and GT1-motif), anaerobic induction (ARE), abscisic acid responsiveness (ABRE), and MeJA responsiveness (CGTCA-motif and TGACG-motif), representing 19.2%, 15.6%, 14.5%, and 9.7%, respectively (Supplementary Figure S2; Supplementary Table S2). Some *LsPRXs*, such as *LsPRX31* and *LsPRX32*, shared an identical cis-element pattern. Notably, the P-responsive element P1BS, related to P starvation, was found in 20 *LsPRX* promoter regions (*LsPRX1*, *LsPRX5*, *LsPRX9*, *LsPRX11*, *LsPRX14*, *LsPRX20*, *LsPRX24*, *LsPRX27*, *LsPRX29*, *LsPRX38*, *LsPRX51*, *LsPRX52*, *LsPRX53*, *LsPRX59*, *LsPRX60*, *LsPRX66*, *LsPRX67*, LsPRX75, *LsPRX78*, and *LsPRX89*).

3.3. Chromosomal Distribution and Duplication Events of LsPRX Genes in Lettuce Genome

The genome organization and distribution of *LsPRX* genes across different lettuce chromosomes (n = 9) is illustrated in Figure 2. Of the 91 *LsPRX* genes, 90 are distributed across nine chromosomes with varying frequencies. Chromosomes 5, 4, and 9 contained the highest numbers of *LsPRX* genes, with 19, 13, and 12 genes, respectively. In contrast, chromosomes 7 and 2 presented the fewest, with two and six genes, respectively. In addition, groups I, II, and IV showed dense clusters of *LsPRXs* in chromosomes 1, 4, 5, 6, 8, and 9. Notably, the clusters of group I were located only close to the telomeres of chromosomes 4 and 5 (Figure 2).

The *LsPRX* gene duplication events were also investigated. Among the 91 *LsPRX* genes, 28 pairs were involved in tandem duplication (duplication with proximity below 200 kb), suggesting that tandem duplications significantly contributed to the expansion of the *LsPRX* gene family in lettuce (Supplementary Table S3). On the other hand, seven *LsPRX* pairs, mainly from group I, resulted from whole-genome duplication (*LsPRX15-LsPRX75*, *LsPRX36-LsPRX16*, *LsPRX40-LsPRX17*, *LsPRX19-LsPRX69*, *LsPRX23-LsPRX71*, *LsPRX40-LsPRX35*, and *LsPRX45-LsPRX68*) (Figure 3; Supplementary Table S3).

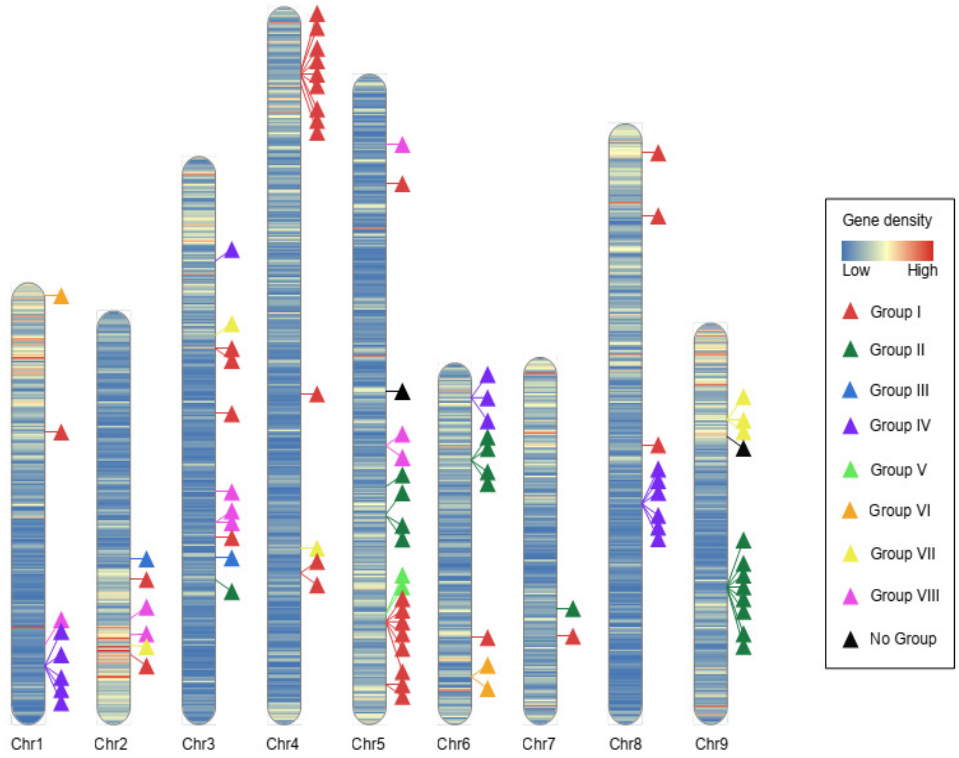

Figure 2. Distribution of the *LsPRX* gene family in the lettuce genome. The segments represent the complete chromosome set of lettuce (n = 9); colors from blue to red indicate gene density per chromosome. The colored triangles corresponding to each group (as determined by phylogenetic analyses, see Figure 1) indicate the location of each *LsPRX* gene on the chromosomes.

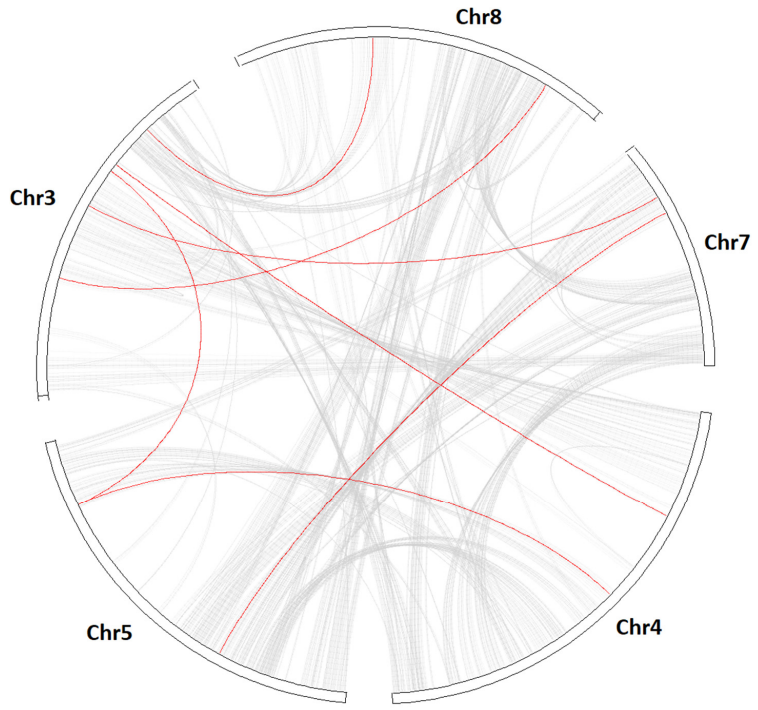

Figure 3. Graphical representation of synteny blocks of lettuce chromosomes containing *LsPRX* genes originating from whole-genome duplication events (red arches) and synteny blocks of other gene pairs (grey arches) on the analyzed chromosomes.

3.4. Phylogenetic and Synteny Analysis of PRXs Among Species

The evolutionary relationships of the LsPRXs with PRXs from other species was assessed by aligning the 91 PRX protein sequences from *L. sativa* with PRXs from *A. thaliana* (AtPRXs), *Z. mays* (ZmPRXs), and *S. tuberosum* (StPRXs) [12,14,43]. The phylogenetic tree evidenced 11 clusters (A–K; Supplementary Figure S3). Cluster F was the largest, containing 95 PRX members: 35 ZmPRXs, 28 StPRXs, 27 LsPRXs, and 5 AtPRXs. Clusters A and H also included a large number of PRXs, containing 58 and 49 members, respectively (Supplementary Figure S3). In particular, 20 and 15 LsPRXs were found in A and H, respectively. In contrast, clusters G, I, and J were the smallest, containing 4, 3, and 12 PRXs. Interestingly, cluster K primarily consisted of ZmPRXs and StPRXs, with only two PRXs from *L. sativa*. Similarly, cluster J mainly comprised ZmPRXs, with just one LsPRX and one StPRX.

The syntenic relationships of *PRX* genes among *L. sativa* and the three other selected species (*A. thaliana*, *S. tuberosum*, and *Z. mays*) were explored to understand the duplication and evolution of the *PRX* gene family in dicotyledons and monocotyledons (Figure 4). The results revealed 39, 28, and 3 syntenic gene pairs of *PRX* genes between lettuce and *S. tuberosum*, lettuce and *A. thaliana*, and lettuce and *Z. mays*, respectively (Figure 4). The majority of orthologous *PRX* gene pairs (35%) in common with *L. sativa* were found in chromosome 5 of *A. thaliana*. Similarly, 46% of the orthologous *PRXs* shared with *L. sativa* were found in chromosome 2 of *S. tuberosum*. Interestingly, 17 orthologous *PRXs* were found in common between *L. sativa* and *A. thaliana* and *S. tuberosum* (Figure 4), whereas three orthologous *LsPRXs* (*LsPRX11*, *LsPRX56*, and *LsPRX70*) were in common among all the species (Figure 4), highlighting their significance in the evolutionary history of this multigene family.

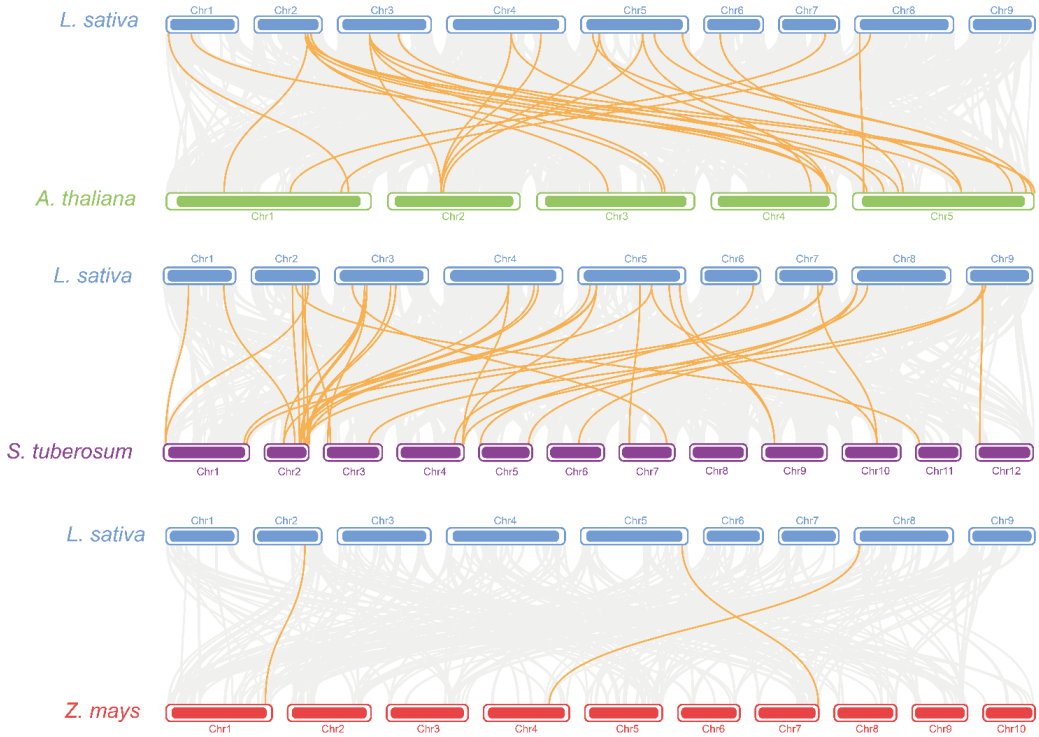

Figure 4. Interspecies synteny of *L. sativa* vs. *A. thaliana*, vs. *S. tuberosum*, and vs. *Z. mays* based on orthologous *LsPRX* genes. Grey lines in the background indicate collinear blocks, while orange lines highlight syntenic *LsPRX* gene pairs.

3.5. Expression Patterns and Gene Network Analysis of LsPRX Genes

The expression patterns of *LsPRX* genes in roots and leaves in lettuces in relation to P (LoP/−AM vs. HiP/−AM) and mycorrhizal (LoP/−AM vs. LoP/+AM) effects were

explored. The tissue-specific expression profiles revealed that the mean expression of all *LsPRX* groups, except for group V, was higher in the root compared to the leaf, independent of the treatment (Supplementary Figure S4; Supplementary Table S4). This could suggest that most *LsPRX* genes play a more critical role in the root than in the leaf. To further investigate the response of *LsPRX* genes to AMS and P supply, the differentially expressed *LsPRX* genes among tissues were identified (Figure 5; Supplementary Table S5; Supplementary Figure S5). Twenty-two *LsPRX* genes were differentially expressed. Fourteen of them, approximately 15% of the total *LsPRX* genes (*LsPRX2*, *LsPRX27*, *LsPRX43*, *LsPRX79*, *LsPRX3*, *LsPRX23*, *LsPRX71*, *LsPRX9*, *LsPRX40*, *LsPRX17*, *LsPRX67*, *LsPRX64*, *LsPRX24*, and *LsPRX77*), exhibited significant downregulation in the root during mycorrhization (LoP/−AM vs. LoP/+AM), hinting at the pivotal role of this gene family in the mycorrhization process during P deprivation (Figure 5; Supplementary Figure S5). Interestingly, 6 of the 14 *LsPRXs* involved in this process in the root belong to group I. Additionally, four *LsPRXs* (*LsPRX71*, *LsPRX85*, *LsPRX56*, and *LsPRX6*) were underexpressed in the root and three were overexpressed (*LsPRX27*, *LsPRX88*, and *LsPRX66*) in the leaf during P supply (LoP/−AM vs. HiP/−AM), while only *LsPRX12* was underexpressed in the leaf during mycorrhization (Figure 5; Supplementary Table S5; Supplementary Figure S5).

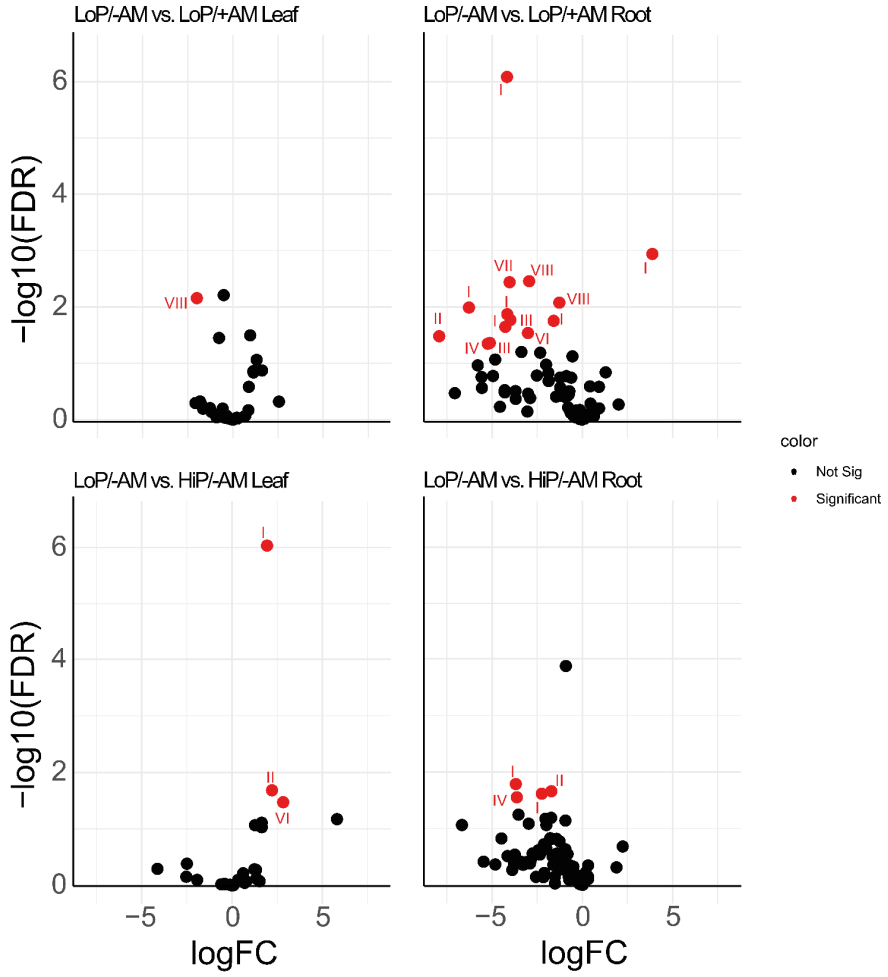

Figure 5. Volcano plots showing *LsPRX* genes expressed in root and leaf under mycorrhization (LoP/−AM vs. LoP/+AM) and phosphorus supply (LoP/−AM vs. HiP/−AM). LoP/+AM = mycorrhized plants with suboptimal phosphorus; HiP/−AM = plants grown with optimal phosphate concentration in nutrient solution and without AMS; LoP/−AM = plants grown with sub-optimal phosphate concentration in nutrient solution and without AMS. Red dots represent differentially expressed *LsPRX* genes, with the roman numbers indicating PRX groups. FC = fold change; FDR = false discovery rate.

Given that most differentially expressed *LsPRX* genes were found in mycorrhized roots (LoP/−AM vs. LoP/+AM), indicating their crucial role in AMS this process, a weighted gene co-expression network analysis (WGCNA) was conducted to identify co-expression modules in lettuce, aiming to detect possible gene networks involving *LsPRX* genes. Overall, the differentially expressed genes were grouped into 11 modules, identified by color clusters (Supplementary Figure S6): black, brown, cyan, green, grey, light cyan, light green, purple, red, tan, and yellow, consisting of 149, 87, 217, 82, 117, 59, 420, 76, 81, 69, and 84 eigengenes, respectively. Interestingly, the core of the light green module (cutoff = 0.75) included 42 eigengenes (Figure 6). Among them, five *LsPRXs* (*LsPRX17*, *LsPRX23*, *LsPRX24*, *LsPRX64*, and *LsPRX79*) were identified. This gene network also included other key eigengenes such as *dirigent protein 11* (*DIR11*) and *dirigent protein 23* (*DIR23*), which are involved in the biosynthesis of lignans; *expansin-A7* (*EXPA7*), which facilitates the loosening and extension of plant cell walls; *laccase-12* (*LAC12*), involved in vascular lignification; *pectinesterase 2* (*PME2*) and *pectinesterase inhibitor 4* (*PMEI4*), both of which are crucial for cell wall modification; two *GDSL esterases/lipases* (*GDL38* and *GDL80*), involved in regulation of plant cell wall components; and *SEED AND ROOT HAIR PROTECTIVE PROTEIN* (*SRPP*), which contributes to cell wall structure in root hairs (Figure 6).

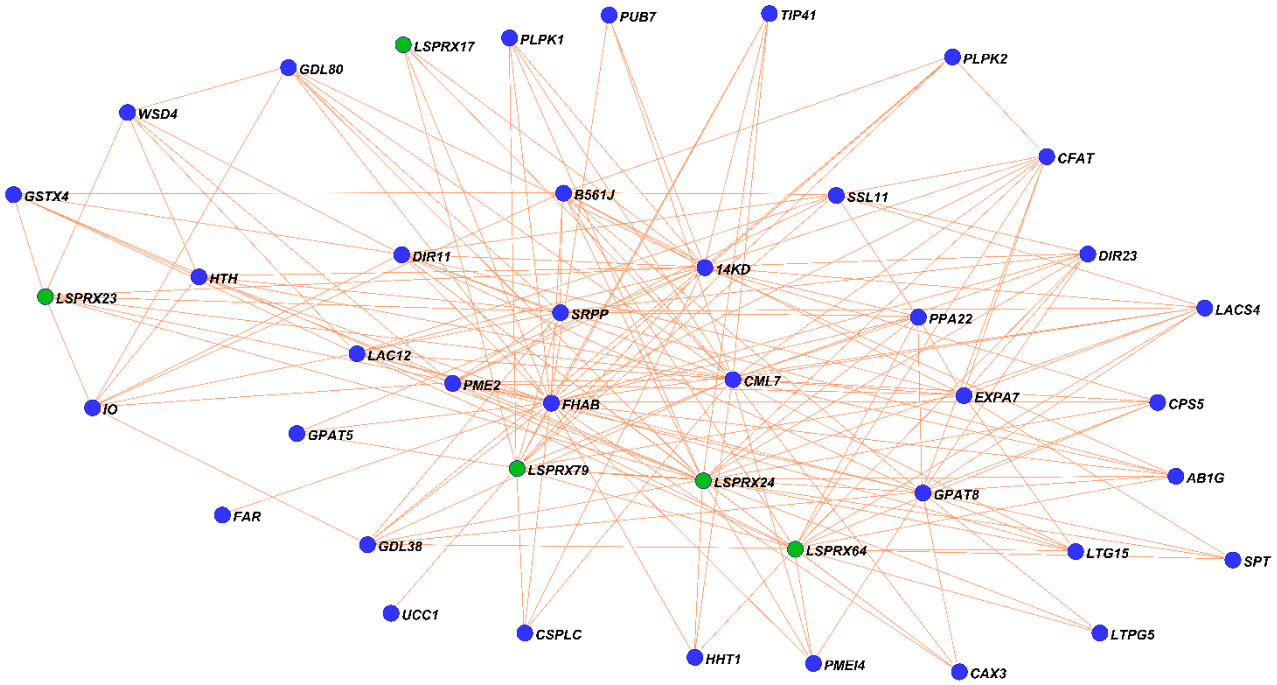

Figure 6. Co-expression gene network of the light green module. The network shows interactions (orange lines) detected between eigengenes in the module, with a cutoff of 0.75. Each node represents a gene within the network. Green dots represent *LsPRX* genes in the gene network.

4. Discussion

4.1. Evolutionary Insights of PRX Gene Family in Lettuce

Class III peroxidases are widely distributed among terrestrial plant species and serve multiple functions, including plant growth, development, and stress responses [54]. To date, a comprehensive genome-wide analysis of the *PRX* gene family has been conducted in several plant species, including potato (102 *PRXs*) [14], carrot (102 *PRXs*) [55], watermelon (79 *PRXs*) [56], soybean (124 *PRXs*) [57], tobacco (210 *PRXs*) [58], and sugarcane (82 *PRXs*) [59]. In this study, a total of 91 *PRX* genes were identified for the first time in lettuce, a number in line with those of carrot, potato, and sugarcane. Lettuce PRX proteins were subdivided into eight groups based on phylogenetic relationships and characterized by gene structure, motif distribution, and cis-element composition analyses, providing a robust and reliable characterization of this multigenic family and considering possible

divergent gene sequences that originated during lettuce genome evolution, similarly to what has been reported in studies of other gene families in plant genomes [60–62]. LsPRX proteins belonging to the same phylogenetic group showed similar intron/exon structure and motif distribution, consistent with other findings, such as in maize [43], potato [14], and carrot [55]. In particular, the model constituted by three introns and four exons found in the majority of *LsPRX* genes also represented a significant proportion in Arabidopsis [12], rice [1] and potato [14], suggesting that it is an ancestral gene structure of *PRX* genes. However, slight variations in intron–exon structure and in few motifs in LsPRX protein groups I, II, and IV suggest that members of the same group may constitute LsPRX subgroups with divergent evolutionary histories [63] and different functions.

Cis-acting elements in *LsPRX* promoter regions were analyzed in the 1000 bp upstream gene region, as they can provide useful information regarding gene function in genome-wide studies [53,62]. Although cis-elements failed to discriminate groups clearly, elements responsive to abiotic stresses and hormones have been found in the *LsPRX* gene family in almost equal frequency. Some *LsPRXs* displayed a similar positioning pattern and number of cis-elements, highlighting the duplication of non-coding regions. Nevertheless, similar cis-element roles in biotic and abiotic stresses for *PRXs* have been found in sugarcane [59], watermelon [56], and tobacco [58]. The P1BS cis-element (GNATATNC) was identified in the promoter region of 20 *LsPRX* genes. Since P starvation activates the function of PHR transcription factors, which regulate the expression of downstream P starvation-responsive genes, the presence of the P1BS motif suggests that these LsPRXs may be directly regulated by PHRs during P starvation [64]. This finding strengthens the hypothesis of LsPRX involvement in P starvation signaling.

Gene duplication events, primarily occurring via segmental, tandem, and whole-genome duplication [65], are crucial for gene family expansion during evolution and plant adaptation [66–68]. These events can produce two gene copies, with one or both acquiring novel functions under reduced selective pressure [69,70]. The genome of Asteraceae, which includes lettuce, evolved over a million-year period through multiple polyploidization events, creating patterns of duplicated genes and chromosome synteny [34,71]. However, in lettuce, several gene families, including ABFs [72], CBF/DREB1 genes [73], AP2/ERF genes [74], and Hsp70s [75], underwent tandem duplication. In our study, 28 *LsPRX* pairs, belonging mainly to groups I, II, and IV, were derived from tandem duplication and were densely distributed in telomeric regions, while 7 pairs were derived from whole-genome duplication. Thus, tandem duplication significantly contributes to the expansion of *LsPRX* genes, similar to what was observed in poplar [76] and *B. distachyon* [53]. In contrast, in tobacco [58], soybean [57], and potato [14], segmental duplication is the main driver for the expansion of the class III *PRX* gene family. Synteny analysis assessed the relationship between *LsPRX* genes and their orthologues in *A. thaliana* and *S. tuberosum*, representing dicots, and *Z. mays*, representing monocots. Notably, 46% of the orthologous *PRXs* shared with *L. sativa* are found on chromosome 2 of *S. tuberosum*, where the most significant number of *StPRX* genes were located [14]. The number of orthologous genes shared between *L. sativa* and *S. tuberosum* was the highest, suggesting the closest evolutionary relationship, followed by *A. thaliana* and *Z. mays*. The identification of three orthologous *LsPRXs* (*LsPRX11*, *LsPRX56*, and *LsPRX70*) shared by both monocots and dicots suggests that these *LsPRX* genes are likely to serve fundamental roles preserved during the divergence of these major groups of plants. Overall, these results support the hypothesis that large-scale duplication events occurring after the divergence of monocots and dicots played a crucial role in expanding the *PRX* gene family.

4.2. Gene Expression Analyses of LsPRXs During Mycorrhizal Symbiosis and Phosphorus Deprivation

In recent years, several studies analyzed the gene expression of *PRXs* in different plant organs and response to biotic and abiotic stress [14,43,77,78]. In this study, we explored the expression patterns of *LsPRXs* in roots and leaves in relation to P (LoP/−AM vs. HiP/−AM)

and mycorrhizal (LoP/−AM vs. LoP/+AM) conditions in lettuce. The analysis of organ-specific expression profiles showed that the average expression level of almost all LsPRX groups is higher in the roots compared to the leaves, regardless of the culture conditions. Similar findings have been reported in potato [14], maize [13], Arabidopsis [12], and rice [1], suggesting that the PRX family is pivotal for root function in plants. Notably, the absence of expression in the roots or leaves of *PRXs* from group V suggests that they could be specific to other plant tissues or could be expressed in different developmental stages or in response to other effectors. To better understand the potential functions of the *LsPRX* genes in AMS and P supply in lettuce, we conducted a differential expression analysis of *LsPRXs* in root and leaf. Interestingly, 15% of the total *PRXs* in lettuce were found to be regulated in the root during mycorrhization under P deficiency.

During the arbuscular formation and cell–fungus approach, the mycorrhizal symbiotic interaction is linked with a modification of the cell wall structure [78], altering root enzymes, including peroxidase activity [79]. Nevertheless, numerous class III PRX isoforms are present in the cell wall [80–82] to specifically control the relationship between cell wall loosening and stiffening by acting on cross-links of polysaccharides [83,84]. PRXs are also known to be activated in response to pathogen attacks, and several roles have been attributed to plant PRXs in host–pathogen interaction [54,79], where oxidative bursts characterized by massive ROS production generated by PRX activity can lead to a highly toxic environment, resulting in adverse growth conditions for microorganisms. As a matter of fact, during symbiosis, the plant initially activates a pathogen response, which then diminishes to facilitate plant–AMS interaction [85].

A total of four and three *LsPRXs* were differentially expressed during P supply in the root and leaf, respectively. It is a matter of fact that PRXs have a crucial role during P starvation [86]. Nevertheless, several studies indicated that biotic and abiotic stresses stimulate the activity of PRXs, activating the balancing between cell wall expansion and stiffening [15,87,88]. Notably, *LsPRX71* was differentially expressed in root during both AMS and P supply, suggesting its multifunctional role in both treatments. Amongst all differentially expressed *LsPRXs*, only *LsPRX56* had orthologues in the other species, and its contribution during P supply in root could represent an early evolutionary attempt of stress response from class III PRXs.

The highest number of differentially expressed *LsPRXs* was found during root mycorrhization under P deficiency, indicating their importance in this biological process. A weighted gene co-expression network analysis (WGCNA) on differentially expressed genes allowed us to elucidate the gene network involved. The core of highly correlated genes in the module included five *LsPRXs* (*LsPRX17*, *LsPRX23*, *LsPRX24*, *LsPRX64*, and *LsPRX79*) and many key genes related to cell wall reorganization and remodeling during mycorrhization. *Dirigent protein 11* (*DIR11*) and *dirigent protein 23* (*DIR23*) are specific monolignol (radical) binding proteins that influence the formation of optically active lignans in the biosynthesis of lignans [89,90]. Various *DIR* genes are expressed during wounding and pathogen infection, suggesting their involvement in pathogen defense [91]. They were also found to be regulated in mycorrhized roots [92]. *Expansin-A7* (*EXPA7*) contributes to the loosening and extending of plant cell walls by suppressing hydrogen bonds between cellulose and xyloglucan [93] and was found to be differentially regulated in mycorrhized roots [94]. Laccases (LACs) and class III peroxidases are involved in the final step of lignin deposition in the cell wall through the oxidative polymerization of phenolic monomers [95]. Specific *LACs* are required to accumulate specific lignins, and *laccase-12* (*LAC12*) plays a crucial role in vascular lignification [96]. Nevertheless, the expression of *LAC* genes in plants can be influenced by the colonization of AM fungi in species such as pea and wheat [97–99]. *Pectinesterase 2* (*PME2*) participates in the modification of the structural characteristics of the cell wall by altering the methylesterification status of the pectin network [100], while *Pectinesterase inhibitor 4* (*PMEI4*) regulates this process, affecting root growth [101]. Two *GDSL esterase/lipase* (*GDL38* and *GDL80*) genes were also found in the network. *GDSL-type esterases/lipases* are related to morphological development, abiotic stress response, pathogen

defense [102], and regulation of plant cell wall components [103]. Their significant expression in arbuscular cells during AMS has been linked to the production of signaling molecules and membrane components essential for the synthesis of periarbuscular membranes [26,27]. Moreover, it has been shown that *SEED AND ROOT HAIR PROTECTIVE PROTEIN* (*SRPP*) maintains the structure and function of root hairs and contributes to constructing robust cell walls [104]. The association of *LsPRXs* in this gene network during mycorrhizal symbiosis indicates that these genes are crucial for facilitating and sustaining the symbiotic relationship by modifying root architecture and cell wall structure in conjunction with the modulation of the immune response initially activated against mycorrhizal fungi. Overall, our analysis strongly correlates the expression of five *LsPRXs* with several genes related to remodeling and reorganization during mycorrhization, expanding the knowledge of the gene network involved during this process.

5. Conclusions

In this study, we conducted the first genome-wide investigation and comprehensive analysis of the class III peroxidase family in lettuce. The 91 identified members of this family were categorized into eight groups based on phylogenetic relationships and characterized by gene structure, motif distribution, and regulatory cis-element composition. Evolutionary analysis indicated that large-scale tandem duplications, occurring after the divergence of monocots and dicots, were the main drivers of PRX family expansion in lettuce. Expression analyses showed that 15% of the total *LsPRXs* are differentially expressed in roots during mycorrhization, suggesting their pivotal role in this process. Amongst these, five *LsPRX* genes (*LsPRX17*, *LsPRX23*, *LsPRX24*, *LsPRX64*, and *LsPRX79*) were found in a network of highly correlated genes involved in cell wall reorganization and remodeling during mycorrhization. Our results offer valuable insights into the evolutionary history and functional roles of *PRX* genes in lettuce. Additionally, our work identifies candidate gene targets that may play a role in the bio-stimulant effects of arbuscular symbiosis, aiding in coping with phosphorus deficiency.

Supplementary Materials: The following supporting information can be downloaded at: https://www.mdpi.com/article/10.3390/horticulturae10111170/s1, Figure S1: Legend of Figure 1. (a) exon (green) and intron (black dash) structure produced by GSDS; (b) structural motifs identified on protein sequences by MEME; (c) cis-acting elements in the 1000 bp upstream region of *LsPRX* genes predicted by PlantCare; Figure S2: The heatmap of cis-elements shared among 91 *LsPRXs*; Figure S3: Phylogenetic tree of PRX protein sequences from *L. sativa*, *A. thaliana*, *Z. mays*, and *S. tuberosum*, constructed using the maximum likelihood method. * indicates Bootstrap values above 60%; Figure S4: Expression values, as the square root of RPKM, for each LsPRX group (number on the right) in root and leaf during mycorrhization and phosphorus supply. LoP/+AM= mycorrhizal plants; HiP/−AM= plants grown with optimal phosphate concentration in nutrient solution; LoP/−AM= plants grown with sub-optimal phosphate concentration in nutrient solution. For each treatment, the average square root RPKM value is reported; Figure S5: barchart showing *LsPRX* genes differentially expressed in root and leaf under mycorrhization (LoP/−AM vs. LoP/+AM) and phosphorus supply (LoP/−AM vs. HiP/−AM). LoP/+AM= mycorrhized plants with suboptimal phosphorus according to their FC = fold change; HiP/−AM= plants grown with optimal phosphate concentration in nutrient solution and without AMS; LoP/−AM= plants grown with sub-optimal phosphate concentration in nutrient solution and without AMS; Figure S6: Hierarchical cluster dendrogram showing correlation modules identified by WGCNA with minModuleSize = 50 and MEDissThres = 0.09. Each colored row represents a module containing a group of highly connected genes. Table S1: ST1; Table S2: ST2; Table S3: ST3; Table S4: ST4; Table S5: ST5; Supplementary Data S1: complete amino acid sequences of LsPRXs; Supplementary Data S2: complete CDS sequences of LsPRXs.

Author Contributions: Conceptualization, A.V. and A.C.; data curation, S.S., M.C., G.U., U.R., F.M., T.G. and L.N.; investigation, S.S. and M.C.; methodology, S.S., M.C., A.V., A.C., G.U., U.R., F.M., T.G. and L.N.; writing—original draft, S.S.; writing—review and editing, all authors have contributed. All authors have read and agreed to the published version of the manuscript.

Funding: This research received no external funding.

Data Availability Statement: Publicly available datasets were analyzed in this study. These data can be found here: https://www.ncbi.nlm.nih.gov/ (accessed on 22 January 2024).

Conflicts of Interest: The authors declare no conflict of interest.

References

1. Passardi, F.; Penel, C.; Dunand, C. Performing the paradoxical: How plant peroxidases modify the cell wall. *Trends Plant Sci.* **2004**, *9*, 534–540. [CrossRef]
2. Sellami, K.; Couvert, A.; Nasrallah, N.; Maachi, R.; Abouseoud, M.; Amrane, A. Peroxidase enzymes as green catalysts for bioremediation and biotechnological applications: A review. *Sci. Total Environ.* **2022**, *806*, 150500. [CrossRef] [PubMed]
3. Pandey, V.P.; Awasthi, M.; Singh, S.; Tiwari, S.; Dwivedi, U.N. A Comprehensive Review on Function and Application of Plant Peroxidases. *Biochem. Anal. Biochem.* **2017**, *6*, 308. [CrossRef]
4. Shigeoka, S.; Ishikawa, T.; Tamoi, M.; Miyagawa, Y.; Takeda, T.; Yabuta, Y.; Yoshimura, K. Regulation and function of ascorbate peroxidase isoenzymes. *J. Exp. Bot.* **2002**, *53*, 1305–1319. [CrossRef] [PubMed]
5. Martínez, A.T.; Speranza, M.; Ruiz-Dueñas, F.J.; Ferreira, P.; Camarero, S.; Guillén, F.; Martínez, M.J.; Gutiérrez, A.; del Río, J.C. Biodegradation of lignocellulosics: Microbial, chemical, and enzymatic aspects of the fungal attack of lignin. *Int. Microbiol.* **2005**, *8*, 195–204. [PubMed]
6. Kidwai, M.; Ahmad, I.Z.; Chakrabarty, D. Class III peroxidase: An indispensable enzyme for biotic/abiotic stress tolerance and a potent candidate for crop improvement. *Plant Cell Rep.* **2020**, *39*, 1381–1393. [CrossRef]
7. Cosio, C.; Dunand, C. Specific functions of individual class III peroxidase genes. *J. Exp. Bot.* **2009**, *60*, 391–408. [CrossRef]
8. Barceló, A.R.; Pomar, F. Oxidation of cinnamyl alcohols and aldehydes by a basic peroxidase from lignifying Zinnia elegans hypocotyls. *Phytochemistry* **2001**, *57*, 1105–1113. [CrossRef]
9. Gazaryan, I.G.; Lagrimini, L.M.; Ashby, G.A.; Thorneley, R.N. Mechanism of indole-3-acetic acid oxidation by plant peroxidases: Anaerobic stopped-flow spectrophotometric studies on horseradish and tobacco peroxidases. *Biochem. J.* **1996**, *313*, 841–847. [CrossRef]
10. McInnis, S.M.; Desikan, R.; Hancock, J.T.; Hiscock, S.J. Production of reactive oxygen species and reactive nitrogen species by angiosperm stigmas and pollen: Potential signalling crosstalk? *New Phytol.* **2006**, *172*, 221–228. [CrossRef]
11. Bindschedler, L.V.; Dewdney, J.; Blee, K.A.; Stone, J.M.; Asai, T.; Plotnikov, J.; Denoux, C.; Hayes, T.; Gerrish, C.; Davies, D.R.; et al. Peroxidase-dependent apoplastic oxidative burst in Arabidopsis required for pathogen resistance. *Plant J.* **2006**, *47*, 851–863. [CrossRef] [PubMed]
12. Tognolli, M.; Penel, C.; Greppin, H.; Simon, P. Analysis and expression of the class III peroxidase large gene family in Arabidopsis thaliana. *Gene* **2002**, *288*, 129–138. [CrossRef] [PubMed]
13. Wang, C.-J.; Chan, Y.-L.; Shien, C.H.; Yeh, K.-W. Molecular characterization of fruit-specific class III peroxidase genes in tomato (*Solanum lycopersicum*). *J. Plant Physiol.* **2015**, *177*, 83–92. [CrossRef] [PubMed]
14. Yang, X.; Yuan, J.; Luo, W.; Qin, M.; Yang, J.; Wu, W.; Xie, X. Genome-Wide Identification and Expression Analysis of the Class III Peroxidase Gene Family in Potato (*Solanum tuberosum* L.). *Front. Genet.* **2020**, *11*, 593577. [CrossRef]
15. Zhang, X.; Hu, W.; Xie, X.; Wu, Y.; Liang, F.; Tang, M. Arbuscular mycorrhizal fungi promote lead immobilization by increasing the polysaccharide content within pectin and inducing cell wall peroxidase activity. *Chemosphere* **2021**, *267*, 128924. [CrossRef]
16. Vance, C.P.; Uhde-Stone, C.; Allan, D.L. Phosphorus acquisition and use: Critical adaptations by plants for securing a nonrenewable resource. *New Phytol.* **2003**, *157*, 423–447. [CrossRef]
17. Plaxton, W.C.; Lambers, H. (Eds.) *Annual Plant Reviews Volume 48: Phosphorus Metabolism in Plants*; Wiley: Hoboken, NJ, USA, 2015; ISBN 9781118958858.
18. Dissanayaka, D.M.S.B.; Ghahremani, M.; Siebers, M.; Wasaki, J.; Plaxton, W.C. Recent insights into the metabolic adaptations of phosphorus-deprived plants. *J. Exp. Bot.* **2021**, *72*, 199–223. [CrossRef]
19. Malhotra, H.; Vandana; Sharma, S.; Pandey, R. Phosphorus Nutrition: Plant Growth in Response to Deficiency and Excess. In *Plant Nutrients and Abiotic Stress Tolerance*; Springer: Singapore, 2018; pp. 171–190.
20. Li, Y.; Steenwyk, J.L.; Chang, Y.; Wang, Y.; James, T.Y.; Stajich, J.E.; Spatafora, J.W.; Groenewald, M.; Dunn, C.W.; Hittinger, C.T.; et al. A genome-scale phylogeny of the kingdom Fungi. *Curr. Biol.* **2021**, *31*, 1653–1665.e5. [CrossRef]
21. Smith, S.E.; Read, D.J. *Mycorrhizal Symbiosis*; Elsevier: Amsterdam, The Netherlands, 2008; ISBN 9780123705266.
22. Avio, L.; Sbrana, C.; Giovannetti, M.; Frassinetti, S. Arbuscular mycorrhizal fungi affect total phenolics content and antioxidant activity in leaves of oak leaf lettuce varieties. *Sci. Hortic.* **2017**, *224*, 265–271. [CrossRef]
23. Evelin, H.; Devi, T.S.; Gupta, S.; Kapoor, R. Mitigation of Salinity Stress in Plants by Arbuscular Mycorrhizal Symbiosis: Current Understanding and New Challenges. *Front. Plant Sci.* **2019**, *10*, 470. [CrossRef]
24. Feng, J.; Lv, W.; Xu, J.; Huang, Z.; Rui, W.; Lei, X.; Ju, X.; Li, Z. Overlapping Root Architecture and Gene Expression of Nitrogen Transporters for Nitrogen Acquisition of Tomato Plants Colonized with Isolates of *Funneliformis mosseae* in Hydroponic Production. *Plants* **2022**, *11*, 1176. [CrossRef] [PubMed]
25. Germano, R.P.; Melito, S.; Cacini, S.; Carmassi, G.; Leoni, F.; Maggini, R.; Montesano, F.F.; Pardossi, A.; Massa, D. Sweet basil can be grown hydroponically at low phosphorus and high sodium chloride concentration: Effect on plant and nutrient solution management. *Sci. Hortic.* **2022**, *304*, 111324. [CrossRef]

26. Vangelisti, A.; Natali, L.; Bernardi, R.; Sbrana, C.; Turrini, A.; Hassani-Pak, K.; Hughes, D.; Cavallini, A.; Giovannetti, M.; Giordani, T. Transcriptome changes induced by arbuscular mycorrhizal fungi in sunflower (*Helianthus annuus* L.) roots. *Sci. Rep.* **2018**, *8*, 4. [CrossRef] [PubMed]
27. Handa, Y.; Nishide, H.; Takeda, N.; Suzuki, Y.; Kawaguchi, M.; Saito, K. RNA-seq Transcriptional Profiling of an Arbuscular Mycorrhiza Provides Insights into Regulated and Coordinated Gene Expression in Lotus japonicus and *Rhizophagus irregularis*. *Plant Cell Physiol.* **2015**, *56*, 1490–1511. [CrossRef] [PubMed]
28. Puccio, G.; Ingraffia, R.; Mercati, F.; Amato, G.; Giambalvo, D.; Martinelli, F.; Sunseri, F.; Frenda, A.S. Transcriptome changes induced by Arbuscular mycorrhizal symbiosis in leaves of durum wheat (*Triticum durum Desf.*) promote higher salt tolerance. *Sci. Rep.* **2023**, *13*, 116. [CrossRef]
29. Zouari, I.; Salvioli, A.; Chialva, M.; Novero, M.; Miozzi, L.; Tenore, G.C.; Bagnaresi, P.; Bonfante, P. From root to fruit: RNA-Seq analysis shows that arbuscular mycorrhizal symbiosis may affect tomato fruit metabolism. *BMC Genom.* **2014**, *15*, 221. [CrossRef]
30. Cela, F.; Avio, L.; Giordani, T.; Vangelisti, A.; Cavallini, A.; Turrini, A.; Sbrana, C.; Pardossi, A.; Incrocci, L. Arbuscular Mycorrhizal Fungi Increase Nutritional Quality of Soilless Grown Lettuce while Overcoming Low Phosphorus Supply. *Foods* **2022**, *11*, 3612. [CrossRef]
31. Vangelisti, A.; Simoni, S.; Cela, F.; Avio, L.; Turrini, A.; Sbrana, C.; Incrocci, L.; Pardossi, A.; Usai, G.; Mascagni, F.; et al. Arbuscular symbiosis affects transcriptomic regulation of primary metabolism in leaves of soilless cultivated lettuces. *Agrochimica* **2023**, *67*, 75–84. [CrossRef]
32. Vangelisti, A.; Cela, F.; Simoni, S.; Avio, L.; Turrini, A.; Sbrana, C.; Incrocci, L.; Pardossi, A.; Rogo, U.; Natali, L.; et al. Arbuscular mycorrhizal symbiosis allows to overcome phosphorus deficiency in soilless culture of Lactuca sativa: A phenotypic and transcriptomic analysis. *Sci. Hortic.* **2024**, *334*, 113324. [CrossRef]
33. Das, R.; Bhattacharjee, C. Lettuce. In *Nutritional Composition and Antioxidant Properties of Fruits and Vegetables*; Elsevier: Amsterdam, The Netherlands, 2020; pp. 143–157.
34. Reyes-Chin-Wo, S.; Wang, Z.; Yang, X.; Kozik, A.; Arikit, S.; Song, C.; Xia, L.; Froenicke, L.; Lavelle, D.O.; Truco, M.-J.; et al. Genome assembly with in vitro proximity ligation data and whole-genome triplication in lettuce. *Nat. Commun.* **2017**, *8*, 14953. [CrossRef]
35. Berardini, T.Z.; Reiser, L.; Li, D.; Mezheritsky, Y.; Muller, R.; Strait, E.; Huala, E. The Arabidopsis information resource: Making and mining the "gold standard" annotated reference plant genome. *Genesis* **2015**, *53*, 474–485. [CrossRef] [PubMed]
36. Altschul, S.F.; Gish, W.; Miller, W.; Myers, E.W.; Lipman, D.J. Basic local alignment search tool. *J. Mol. Biol.* **1990**, *215*, 403–410. [CrossRef] [PubMed]
37. Apweiler, R.; Attwood, T.K.; Bairoch, A.; Bateman, A.; Birney, E.; Biswas, M.; Bucher, P.; Cerutti, L.; Corpet, F.; Croning, M.D.; et al. The InterPro database, an integrated documentation resource for protein families, domains and functional sites. *Nucleic Acids Res.* **2001**, *29*, 37–40. [CrossRef] [PubMed]
38. Kumar, S.; Stecher, G.; Li, M.; Knyaz, C.; Tamura, K. MEGA X: Molecular Evolutionary Genetics Analysis across Computing Platforms. *Mol. Biol. Evol.* **2018**, *35*, 1547–1549. [CrossRef]
39. Bailey, T.L.; Boden, M.; Buske, F.A.; Frith, M.; Grant, C.E.; Clementi, L.; Ren, J.; Li, W.W.; Noble, W.S. MEME SUITE: Tools for motif discovery and searching. *Nucleic Acids Res.* **2009**, *37*, W202–W208. [CrossRef]
40. Lescot, M.; Déhais, P.; Thijs, G.; Marchal, K.; Moreau, Y.; Van de Peer, Y.; Rouzé, P.; Rombauts, S. PlantCARE, a database of plant cis-acting regulatory elements and a portal to tools for in silico analysis of promoter sequences. *Nucleic Acids Res.* **2002**, *30*, 325–327. [CrossRef]
41. Wang, Y.; Tang, H.; Debarry, J.D.; Tan, X.; Li, J.; Wang, X.; Lee, T.; Jin, H.; Marler, B.; Guo, H.; et al. MCScanX: A toolkit for detection and evolutionary analysis of gene synteny and collinearity. *Nucleic Acids Res.* **2012**, *40*, e49. [CrossRef]
42. Hao, Z.; Lv, D.; Ge, Y.; Shi, J.; Weijers, D.; Yu, G.; Chen, J. RIdeogram: Drawing SVG graphics to visualize and map genome-wide data on the idiograms. *PeerJ Comput. Sci.* **2020**, *6*, e251. [CrossRef]
43. Wang, Y.; Wang, Q.; Zhao, Y.; Han, G.; Zhu, S. Systematic analysis of maize class III peroxidase gene family reveals a conserved subfamily involved in abiotic stress response. *Gene* **2015**, *566*, 95–108. [CrossRef]
44. Chen, C.; Chen, H.; Zhang, Y.; Thomas, H.R.; Frank, M.H.; He, Y.; Xia, R. TBtools: An Integrative Toolkit Developed for Interactive Analyses of Big Biological Data. *Mol. Plant* **2020**, *13*, 1194–1202. [CrossRef]
45. Bolger, A.M.; Lohse, M.; Usadel, B. Trimmomatic: A flexible trimmer for Illumina sequence data. *Bioinformatics* **2014**, *30*, 2114–2120. [CrossRef] [PubMed]
46. Quast, C.; Pruesse, E.; Yilmaz, P.; Gerken, J.; Schweer, T.; Yarza, P.; Peplies, J.; Glöckner, F.O. The SILVA ribosomal RNA gene database project: Improved data processing and web-based tools. *Nucleic Acids Res.* **2013**, *41*, D590–D596. [CrossRef] [PubMed]
47. Mortazavi, A.; Williams, B.A.; McCue, K.; Schaeffer, L.; Wold, B. Mapping and quantifying mammalian transcriptomes by RNA-Seq. *Nat. Methods* **2008**, *5*, 621–628. [CrossRef] [PubMed]
48. Robinson, M.D.; McCarthy, D.J.; Smyth, G.K. EdgeR: A Bioconductor package for differential expression analysis of digital gene expression data. *Bioinformatics* **2010**, *26*, 139–140. [CrossRef]
49. Benjamini, Y.; Hochberg, Y. Controlling the False Discovery Rate: A Practical and Powerful Approach to Multiple Testing. *J. R. Stat. Soc. Ser. B Stat. Methodol.* **1995**, *57*, 289–300. [CrossRef]
50. Langfelder, P.; Horvath, S. WGCNA: An R package for weighted correlation network analysis. *BMC Bioinform.* **2008**, *9*, 559. [CrossRef]

51. Hu, Z.; Mellor, J.; Wu, J.; DeLisi, C. VisANT: An online visualization and analysis tool for biological interaction data. *BMC Bioinform.* **2004**, *5*, 17. [CrossRef]
52. Mbadinga Mbadinga, D.L.; Li, Q.; Ranocha, P.; Martinez, Y.; Dunand, C. Global analysis of non-animal peroxidases provides insights into the evolution of this gene family in the green lineage. *J. Exp. Bot.* **2020**, *71*, 3350–3360. [CrossRef]
53. Zhu, T.; Xin, F.; Wei, S.; Liu, Y.; Han, Y.; Xie, J.; Ding, Q.; Ma, L. Genome-wide identification, phylogeny and expression profiling of class III peroxidases gene family in *Brachypodium distachyon*. *Gene* **2019**, *700*, 149–162. [CrossRef]
54. Almagro, L.; Gómez Ros, L.V.; Belchi-Navarro, S.; Bru, R.; Ros Barceló, A.; Pedreño, M.A. Class III peroxidases in plant defence reactions. *J. Exp. Bot.* **2009**, *60*, 377–390. [CrossRef]
55. Meng, G.; Fan, W.; Rasmussen, S.K. Characterisation of the class III peroxidase gene family in carrot taproots and its role in anthocyanin and lignin accumulation. *Plant Physiol. Biochem.* **2021**, *167*, 245–256. [CrossRef] [PubMed]
56. Yang, T.; Zhang, P.; Pan, J.; Amanullah, S.; Luan, F.; Han, W.; Liu, H.; Wang, X. Genome-Wide Analysis of the Peroxidase Gene Family and Verification of Lignin Synthesis-Related Genes in Watermelon. *Int. J. Mol. Sci.* **2022**, *23*, 642. [CrossRef] [PubMed]
57. Aleem, M.; Riaz, A.; Raza, Q.; Aleem, M.; Aslam, M.; Kong, K.; Atif, R.M.; Kashif, M.; Bhat, J.A.; Zhao, T. Genome-wide characterization and functional analysis of class III peroxidase gene family in soybean reveal regulatory roles of GsPOD40 in drought tolerance. *Genomics* **2022**, *114*, 45–60. [CrossRef] [PubMed]
58. Cheng, L.; Ma, L.; Meng, L.; Shang, H.; Cao, P.; Jin, J. Genome-Wide Identification and Analysis of the Class III Peroxidase Gene Family in Tobacco (*Nicotiana tabacum*). *Front. Genet.* **2022**, *13*, 916867. [CrossRef] [PubMed]
59. Shang, H.; Fang, L.; Qin, L.; Jiang, H.; Duan, Z.; Zhang, H.; Yang, Z.; Cheng, G.; Bao, Y.; Xu, J.; et al. Genome-wide identification of the class III peroxidase gene family of sugarcane and its expression profiles under stresses. *Front. Plant Sci.* **2023**, *14*, 1101665. [CrossRef]
60. Jain, M.; Tyagi, A.K.; Khurana, J.P. Genome-wide analysis, evolutionary expansion, and expression of early auxin-responsive SAUR gene family in rice (*Oryza sativa*). *Genomics* **2006**, *88*, 360–371. [CrossRef]
61. Caputi, L.; Malnoy, M.; Goremykin, V.; Nikiforova, S.; Martens, S. A genome-wide phylogenetic reconstruction of family 1 UDP-glycosyltransferases revealed the expansion of the family during the adaptation of plants to life on land. *Plant J.* **2012**, *69*, 1030–1042. [CrossRef]
62. Vangelisti, A.; Simoni, S.; Usai, G.; Mascagni, F.; Ventimiglia, M.; Natali, L.; Cavallini, A.; Giordani, T. In Silico Genome-Wide Characterisation of the Lipid Transfer Protein Multigenic Family in Sunflower (*H. annuus* L.). *Plants* **2022**, *11*, 664. [CrossRef]
63. Rogozin, I.B.; Wolf, Y.I.; Sorokin, A.V.; Mirkin, B.G.; Koonin, E. V Remarkable interkingdom conservation of intron positions and massive, lineage-specific intron loss and gain in eukaryotic evolution. *Curr. Biol.* **2003**, *13*, 1512–1517. [CrossRef]
64. Zhou, J.; Hu, Q.; Xiao, X.; Yao, D.; Ge, S.; Ye, J.; Li, H.; Cai, R.; Liu, R.; Meng, F.; et al. Mechanism of phosphate sensing and signaling revealed by rice SPX1-PHR2 complex structure. *Nat. Commun.* **2021**, *12*, 7040. [CrossRef]
65. Panchy, N.; Lehti-Shiu, M.; Shiu, S.-H. Evolution of Gene Duplication in Plants. *Plant Physiol.* **2016**, *171*, 2294–2316. [CrossRef] [PubMed]
66. Cannon, S.B.; Mitra, A.; Baumgarten, A.; Young, N.D.; May, G. The roles of segmental and tandem gene duplication in the evolution of large gene families in Arabidopsis thaliana. *BMC Plant Biol.* **2004**, *4*, 10. [CrossRef] [PubMed]
67. Kondrashov, F.A. Gene duplication as a mechanism of genomic adaptation to a changing environment. *Proc. Biol. Sci.* **2012**, *279*, 5048–5057. [CrossRef] [PubMed]
68. Birchler, J.A.; Yang, H. The multiple fates of gene duplications: Deletion, hypofunctionalization, subfunctionalization, neofunctionalization, dosage balance constraints, and neutral variation. *Plant Cell* **2022**, *34*, 2466–2474. [CrossRef] [PubMed]
69. Van de Peer, Y.; Maere, S.; Meyer, A. The evolutionary significance of ancient genome duplications. *Nat. Rev. Genet.* **2009**, *10*, 725–732. [CrossRef]
70. You, J.; Liu, Z.; Qi, Z.; Ma, Y.; Sun, M.; Su, L.; Niu, H.; Peng, Y.; Luo, X.; Zhu, M.; et al. Regulatory controls of duplicated gene expression during fiber development in allotetraploid cotton. *Nat. Genet.* **2023**, *55*, 1987–1997. [CrossRef]
71. Barker, M.S.; Kane, N.C.; Matvienko, M.; Kozik, A.; Michelmore, R.W.; Knapp, S.J.; Rieseberg, L.H. Multiple paleopolyploidizations during the evolution of the Compositae reveal parallel patterns of duplicate gene retention after millions of years. *Mol. Biol. Evol.* **2008**, *25*, 2445–2455. [CrossRef]
72. Li, Z.; Yang, X.; Li, Z.; Zou, X.; Jiang, C.; Zhu, J.; Zhang, Y.; Han, Y.; Liu, C.; Hao, J. Genome-wide analysis of ABF gene family in lettuce (*Lactuca sativa* L.) reveals the negative roles of LsABF1 in thermally induced bolting. *J. Hortic. Sci. Biotechnol.* **2024**, 1–15. [CrossRef]
73. Park, S.; Shi, A.; Mou, B. Genome-wide identification and expression analysis of the CBF/DREB1 gene family in lettuce. *Sci. Rep.* **2020**, *10*, 5733. [CrossRef]
74. Park, S.; Shi, A.; Meinhardt, L.W.; Mou, B. Genome-wide characterization and evolutionary analysis of the AP2/ERF gene family in lettuce (*Lactuca sativa*). *Sci. Rep.* **2023**, *13*, 21990. [CrossRef]
75. Kim, T.; Samraj, S.; Jiménez, J.; Gómez, C.; Liu, T.; Begcy, K. Genome-wide identification of heat shock factors and heat shock proteins in response to UV and high intensity light stress in lettuce. *BMC Plant Biol.* **2021**, *21*, 185. [CrossRef] [PubMed]
76. Ren, L.-L.; Liu, Y.-J.; Liu, H.-J.; Qian, T.-T.; Qi, L.-W.; Wang, X.-R.; Zeng, Q.-Y. Subcellular Relocalization and Positive Selection Play Key Roles in the Retention of Duplicate Genes of Populus Class III Peroxidase Family. *Plant Cell* **2014**, *26*, 2404–2419. [CrossRef] [PubMed]

77. Yan, J.; Su, P.; Li, W.; Xiao, G.; Zhao, Y.; Ma, X.; Wang, H.; Nevo, E.; Kong, L. Genome-wide and evolutionary analysis of the class III peroxidase gene family in wheat and *Aegilops tauschii* reveals that some members are involved in stress responses. *BMC Genom.* **2019**, *20*, 666. [CrossRef] [PubMed]
78. Yang, J.; Chen, R.; Xiang, X.; Liu, W.; Fan, C. Genome-Wide Identification and Expression Analysis of the Class III Peroxidase Gene Family under Abiotic Stresses in Litchi (*Litchi chinensis Sonn.*). *Int. J. Mol. Sci.* **2024**, *25*, 5804. [CrossRef] [PubMed]
79. Passardi, F.; Cosio, C.; Penel, C.; Dunand, C. Peroxidases have more functions than a Swiss army knife. *Plant Cell Rep.* **2005**, *24*, 255–265. [CrossRef]
80. Zhou, S.; Sauve, R.; Howard, E. Identification of a cell wall peroxidase in red calli of *Prunus incisa* Thunb. *Plant Cell Rep.* **2002**, *21*, 380–384. [CrossRef]
81. Passardi, F.; Tognolli, M.; De Meyer, M.; Penel, C.; Dunand, C. Two cell wall associated peroxidases from Arabidopsis influence root elongation. *Planta* **2006**, *223*, 965–974. [CrossRef]
82. Francoz, E.; Ranocha, P.; Nguyen-Kim, H.; Jamet, E.; Burlat, V.; Dunand, C. Roles of cell wall peroxidases in plant development. *Phytochemistry* **2015**, *112*, 15–21. [CrossRef]
83. Mnich, E.; Bjarnholt, N.; Eudes, A.; Harholt, J.; Holland, C.; Jørgensen, B.; Larsen, F.H.; Liu, M.; Manat, R.; Meyer, A.S.; et al. Phenolic cross-links: Building and de-constructing the plant cell wall. *Nat. Prod. Rep.* **2020**, *37*, 919–961. [CrossRef]
84. Freitas, C.D.T.; Costa, J.H.; Germano, T.A.; Rocha, R.D.O.; Ramos, M.V.; Bezerra, L.P. Class III plant peroxidases: From classification to physiological functions. *Int. J. Biol. Macromol.* **2024**, *263*, 130306. [CrossRef]
85. Nishad, R.; Ahmed, T.; Rahman, V.J.; Kareem, A. Modulation of Plant Defense System in Response to Microbial Interactions. *Front. Microbiol.* **2020**, *11*, 1298. [CrossRef] [PubMed]
86. Cocozza, C.; Bartolini, P.; Brunetti, C.; Miozzi, L.; Pignattelli, S.; Podda, A.; Scippa, G.S.; Trupiano, D.; Rotunno, S.; Brilli, F.; et al. Modulation of class III peroxidase pathways and phenylpropanoids in *Arundo donax* under salt and phosphorus stress. *Plant Physiol. Biochem.* **2022**, *183*, 151–159. [CrossRef] [PubMed]
87. Lin, C.C.; Kao, C.H. Abscisic acid induced changes in cell wall peroxidase activity and hydrogen peroxide level in roots of rice seedlings. *Plant Sci.* **2001**, *160*, 323–329. [CrossRef] [PubMed]
88. Xue, Y.J.; Tao, L.; Yang, Z.M. Aluminum-induced cell wall peroxidase activity and lignin synthesis are differentially regulated by jasmonate and nitric oxide. *J. Agric. Food Chem.* **2008**, *56*, 9676–9684. [CrossRef]
89. Davin, L.B.; Wang, H.B.; Crowell, A.L.; Bedgar, D.L.; Martin, D.M.; Sarkanen, S.; Lewis, N.G. Stereoselective bimolecular phenoxy radical coupling by an auxiliary (dirigent) protein without an active center. *Science* **1997**, *275*, 362–366. [CrossRef]
90. Davin, L.B.; Lewis, N.G. Dirigent proteins and dirigent sites explain the mystery of specificity of radical precursor coupling in lignan and lignin biosynthesis. *Plant Physiol.* **2000**, *123*, 453–462. [CrossRef]
91. Paniagua, C.; Bilkova, A.; Jackson, P.; Dabravolski, S.; Riber, W.; Didi, V.; Houser, J.; Gigli-Bisceglia, N.; Wimmerova, M.; Budínská, E.; et al. Dirigent proteins in plants: Modulating cell wall metabolism during abiotic and biotic stress exposure. *J. Exp. Bot.* **2017**, *68*, 3287–3301. [CrossRef]
92. Marquez, N.; Giachero, M.L.; Gallou, A.; Debat, H.J.; Cranenbrouck, S.; Di Rienzo, J.A.; Pozo, M.J.; Ducasse, D.A.; Declerck, S. Transcriptional Changes in Mycorrhizal and Nonmycorrhizal Soybean Plants upon Infection with the Fungal Pathogen *Macrophomina phaseolina*. *Mol. Plant Microbe Interact.* **2018**, *31*, 842–855. [CrossRef]
93. Cosgrove, D.J. Wall structure and wall loosening. A look backwards and forwards. *Plant Physiol.* **2001**, *125*, 131–134. [CrossRef]
94. Nanjareddy, K.; Arthikala, M.-K.; Gómez, B.-M.; Blanco, L.; Lara, M. Differentially expressed genes in mycorrhized and nodulated roots of common bean are associated with defense, cell wall architecture, N metabolism, and P metabolism. *PLoS ONE* **2017**, *12*, e0182328. [CrossRef]
95. Blaschek, L.; Pesquet, E. Phenoloxidases in Plants-How Structural Diversity Enables Functional Specificity. *Front. Plant Sci.* **2021**, *12*, 754601. [CrossRef] [PubMed]
96. Blaschek, L.; Murozuka, E.; Serk, H.; Ménard, D.; Pesquet, E. Different combinations of laccase paralogs nonredundantly control the amount and composition of lignin in specific cell types and cell wall layers in Arabidopsis. *Plant Cell* **2023**, *35*, 889–909. [CrossRef] [PubMed]
97. Zorin, E.A.; Afonin, A.M.; Kulaeva, O.A.; Gribchenko, E.S.; Shtark, O.Y.; Zhukov, V.A. Transcriptome Analysis of Alternative Splicing Events Induced by Arbuscular Mycorrhizal Fungi (*Rhizophagus irregularis*) in Pea (*Pisum sativum* L.) Roots. *Plants* **2020**, *9*, 1700. [CrossRef] [PubMed]
98. Moradi Tarnabi, Z.; Iranbakhsh, A.; Mehregan, I.; Ahmadvand, R. Impact of arbuscular mycorrhizal fungi (AMF) on gene expression of some cell wall and membrane elements of wheat (*Triticum aestivum* L.) under water deficit using transcriptome analysis. *Physiol. Mol. Biol. Plants* **2020**, *26*, 143–162. [CrossRef]
99. Zhong, X.; Li, M.; Zhang, M.; Feng, Y.; Zhang, H.; Tian, H. Genome-wide analysis of the laccase gene family in wheat and relationship with arbuscular mycorrhizal colonization. *Planta* **2022**, *257*, 15. [CrossRef]
100. Tsakali, A.; Asitzoglou, I.-C.; Basdeki, V.; Podia, V.; Adamakis, I.-D.S.; Giannoutsou, E.; Haralampidis, K. The Role of PME2 and PME3 in Arabidopsis Stomatal Development and Morphology. In Proceedings of the 2nd International Electronic Conference on Plant Sciences—10th Anniversary of Journal Plants, Virtual, 1–15 December 2021; p. 36.
101. Wormit, A.; Usadel, B. The Multifaceted Role of Pectin Methylesterase Inhibitors (PMEIs). *Int. J. Mol. Sci.* **2018**, *19*, 2878. [CrossRef]

102. Lai, C.-P.; Huang, L.-M.; Chen, L.-F.O.; Chan, M.-T.; Shaw, J.-F. Genome-wide analysis of GDSL-type esterases/lipases in Arabidopsis. *Plant Mol. Biol.* **2017**, *95*, 181–197. [CrossRef]
103. de La Torre, F.; Sampedro, J.; Zarra, I.; Revilla, G. AtFXG1, an Arabidopsis gene encoding alpha-L-fucosidase active against fucosylated xyloglucan oligosaccharides. *Plant Physiol.* **2002**, *128*, 247–255. [CrossRef]
104. Tanaka, N.; Uno, H.; Okuda, S.; Gunji, S.; Ferjani, A.; Aoyama, T.; Maeshima, M. SRPP, a Cell Wall Protein is Involved in Development and Protection of Seeds and Root Hairs in *Arabidopsis thaliana*. *Plant Cell Physiol.* **2017**, *58*, 760–769. [CrossRef]

Disclaimer/Publisher's Note: The statements, opinions and data contained in all publications are solely those of the individual author(s) and contributor(s) and not of MDPI and/or the editor(s). MDPI and/or the editor(s) disclaim responsibility for any injury to people or property resulting from any ideas, methods, instructions or products referred to in the content.